



<b>Title</b>	Indian Ocean Dipole and Rainfall Drive a Moran Effect in East Africa Malaria Transmission
<b>Author(s)</b>	Chaves, Luis Fernando; Satake, Akiko; Hashizume, Masahiro; Minakawa, Noboru
<b>Citation</b>	Journal of Infectious Diseases, 205(12), 1885-1891 <a href="https://doi.org/10.1093/infdis/jis289">https://doi.org/10.1093/infdis/jis289</a>
<b>Issue Date</b>	2012-06-15
<b>Doc URL</b>	<a href="http://hdl.handle.net/2115/52659">http://hdl.handle.net/2115/52659</a>
<b>Rights</b>	This is a pre-copy-editing, author-produced PDF of an article accepted for publication in Journal of Infectious Diseases following peer review. The definitive publisher-authenticated version J Infect Dis. (2012) 205 (12): 1885-1891 is available online at: <a href="http://jid.oxfordjournals.org/content/205/12/1885">http://jid.oxfordjournals.org/content/205/12/1885</a>
<b>Type</b>	article (author version)
<b>File Information</b>	JID205-12_1885-1891.pdf



[Instructions for use](#)

1 **Indian Ocean Dipole and Rainfall drive a Moran Effect in East Africa Malaria**  
2 **transmission**

3 Luis Fernando Chaves<sup>1,2\*</sup>, Akiko Satake<sup>1</sup>, Masahiro Hashizume<sup>3</sup>, and Noboru Minakawa<sup>3</sup>

4 <sup>1</sup>Graduate School of Environmental Sciences and Global Center of Excellence program on  
5 Integrated Field Environmental Science, Hokkaido University, Sapporo, Japan

6 <sup>2</sup> Programa de Investigación en Enfermedades Tropicales, Escuela de Medicina Veterinaria,  
7 Universidad Nacional, Heredia, Costa Rica

8 <sup>3</sup>Institute of Tropical Medicine (NEKKEN) and Global Center of Excellence program on  
9 Tropical and Emergent Infectious Diseases, Nagasaki University, Nagasaki, Japan

10 Short title: **Climate and Moran effect in malaria**

11  
12 **Footnote**

13  
14 The authors declare no competing interests and that funding agencies had no role on study  
15 design.

16  
17 **Funding** This work was funded by Japan Society for the Promotion of Science and a Nagasaki  
18 University Cooperative Research Grant.

19  
20 \*corresponding author. Address: Graduate School of Environmental Sciences, Hokkaido  
21 University, Room A701 5-chome, Kita 10-jo Nishi, Kita-ku, Sapporo 060-0810, Hokkaido,  
22 Japan. Phone: +81-11-706-2267. Fax: +81-11-706-4954. Email: [lchaves@ees.hokudai.ac.jp](mailto:lchaves@ees.hokudai.ac.jp)

23  
24 Category: **Major Article**

25 197 Words in the abstract

26 3343 words (including: 26 References + Figure Legends)

27 6 Figures + 1 Table

28 Supplementary data:

29 Detailed methods

30

31 **Abstract**

32 **Background:** Patterns of concerted fluctuation in populations, synchrony, can reveal impacts of  
33 climatic variability on disease dynamics. Here, we examined whether malaria transmission has  
34 been synchronous in an area with a common rainfall regime and sensitive to the Indian Ocean  
35 Dipole (IOD), a global climatic phenomenon affecting weather patterns in East Africa.

36 **Methods:** We studied malaria synchrony in five fifteen year long (1984-1999) monthly time  
37 series that encompass an altitudinal gradient, ~1000m to 2000m, along Lake Victoria Basin. We  
38 quantified the association patterns between rainfall and malaria time series at different altitudes  
39 and across the altitudinal gradient encompassed by the study locations.

40 **Results:** We found a positive seasonal association of rainfall with malaria, which decreased with  
41 altitude. By contrast, IOD and interannual rainfall impacts on interannual disease cycles  
42 increased with altitude. Our analysis revealed a non-decaying synchrony of similar magnitude in  
43 both malaria and rainfall, as expected under a Moran effect, supporting a role for climatic  
44 variability on malaria epidemics frequency, which might reflect rainfall mediated changes in  
45 mosquito abundance.

46 **Conclusion:** Synchronous malaria epidemics call for the integration of knowledge on the forcing  
47 of malaria transmission by environmental variability to develop robust malaria control and  
48 elimination programs.

49 **Key-words:** Synchrony, Climate Change, Indian Ocean Dipole, *Anopheles*, *Plasmodium*, Time  
50 Series

51 Synchrony, the degree of concerted fluctuations among populations in a region, is a key  
52 parameter to understand impacts of climatic trends and variability on population dynamics [1].  
53 For infectious diseases, synchrony has become especially important because its estimation offers  
54 a mean to test hypothesis regarding the importance of exogenous epidemic drivers. In a relatively  
55 homogenous environment, a synchrony decay with distance implies that impacts of climatic  
56 trends and variability, if any, are marginal when compared with regulatory factors related to  
57 population processes, e.g., immunity in diseases, and independent of the changing environment  
58 [2]. By contrast, a non-decaying synchrony, of magnitude slightly larger, or similar, to that of the  
59 environment, will support a Moran effect, where transmission patterns in a region could be  
60 similar by a common mechanism of action for the exogenous, often climatic, forcing [3]. As  
61 originally defined, the Moran effect arises by the emerging synchronization of autoregressive  
62 dynamics of time series by the impact of common sources of exogenous forcing, i.e., the  
63 autonomous (or endogenous) dynamics of a population get tuned to that of external factors  
64 influencing the dynamics of populations living under a similar (or correlated) environment [2].

65 Vector-borne diseases, such as malaria, are excellent model systems to study synchrony and test  
66 Moran effects. For example, Moran effects are expected in malaria because of the monotonic  
67 relationship between vector abundance and transmission [4], and between vectors and rainfall  
68 [5]. Lake Victoria basin (LVB) is a unique setting to study exogenous forcing in malaria  
69 transmission because of three main reasons: (i) it encompasses an altitudinal gradient, which is  
70 also a gradient of malaria endemicity [6, 7]; (ii) it has relatively homogeneous rainfall patterns  
71 [8]; (iii) rainfall and malaria are impacted by global climatic phenomena, especially the Indian  
72 Ocean Dipole, an irregular oscillation of sea-surface temperatures in which the western Indian  
73 Ocean becomes alternately warmer and then colder than the eastern part of the ocean [9, 10].

74 Here, we studied malaria synchrony in five fifteen year long (1984-1999) monthly time series  
75 (Fig. 1A) from Lake Victoria basin, West Kenya (Fig. 2). We also studied rainfall time series  
76 (Fig. 1B) synchrony to test the condition of environmental autocorrelation necessary for a Moran  
77 effect. We used the dipole mode index, DMI, (Fig. 1C) as an IOD index [11] to quantify its role  
78 as interannual driver of malaria and rainfall dynamics. We found that both rainfall and malaria  
79 had a non-decaying synchrony with distance, and that malaria synchrony was slightly larger than

80 rainfall synchrony, as expected under a Moran effect. A more detailed time scale analysis of  
81 synchrony showed that seasonal cycles in malaria transmission were led by two month lagged  
82 changes in rainfall, with decreasing intensity as a function of altitude. By contrast, interannual  
83 cycles in the disease were driven by IOD, with an increasing intensity with altitude. These  
84 patterns could be related to the population dynamics of *Anopheles* mosquitoes, whose abundance  
85 is likely driven by rainfall patterns in the region [5, 12]. Finally, our results clearly show that  
86 patterns of climatic variability have a strong signature in malaria transmission among vulnerable  
87 populations, and are, therefore, a necessary input for a strong malaria control/elimination  
88 framework.

## 89 **Materials and Methods**

90 **Data** Malaria and rainfall data spanned from January 1985 to December 1999. The five malaria  
91 time series were monthly counts of inpatients admitted into the hospitals because of high fever  
92 and other clinical malaria symptoms. In Kericho, all malaria cases were confirmed by blood slide  
93 examination [13]. In the other four sites (Maseno, Kendu Bay, Kisii and Kapsabet) we collected  
94 the data from books with malaria diagnosed inpatient records. Unfortunately, these books did not  
95 indicate whether all recorded malaria cases were confirmed by blood slide examination.  
96 However, we were informed by staff members from each hospital that cases were often  
97 confirmed by blood slide examination. We restricted our samples to this kind of malaria  
98 infections, i.e., inpatient admissions, in order to make a sound statistical analysis at the price of  
99 using data that likely underestimate the total number of malaria infections [14]. Rainfall data  
100 were obtained from the Kenyan Meteorological service. We use rainfall records from some of  
101 the same locations of the malaria time series and a location midway between the two lowest  
102 altitude sites (Fig. 2). Specifically, we employ meteorological records from Kisumu as proxy  
103 inputs for Kendu Bay and Maseno, localities for which we were unable to find relatively  
104 complete records through the Kenyan Meteorological services and other meteorological data  
105 repositories. We chose Kisumu because of the lack of missing observations during the study  
106 period, and by the similar rainfall patterns to Kendu Bay and Maseno according to  
107 meteorological models [8].

108 **Statistical Analysis** To estimate synchrony in the time series first we removed non-stationary  
109 trends [15] in the malaria time series(Fig. 1D) using three standard procedures: local polynomial  
110 regression fitting (Loess) [15], singular spectrum analysis (SSA) [16] and the empirical mode  
111 decomposition (EMD) [17]. These methods have different assumptions and outcomes, Loess  
112 extracts (non)linear trends (Fig. 1E), while SSA (Fig. 1F) and EMD decompose signals into  
113 different oscillatory (Fig. 1G, 1H and 1I) and non-cyclical components. In SSA the trends are  
114 extracted by examining the variability of the largest eigenvalue from an autocovariance matrix,  
115 while EMD decomposes a time series by building oscillatory signals, Intrinsic Mode Functions  
116 (IMF), that are repeatedly subtracted from the time series. We employed these different methods  
117 to ensure robustness in the inferences from subsequent analyses. The lack of non-stationary  
118 trends in rainfall made unnecessary the treatment with Loess and SSA. However, we  
119 decomposed rainfall data using EMD to perform frequency specific association analysis (Fig. 3).  
120 Second, we estimated the synchrony,  $r_0$ , i.e., cross correlation at lag 0, of rainfall and detrended  
121 malaria time series, using both linear regression [2] and spline correlogram on high frequency  
122 filtered, detrended time series [18]. Third, we studied the association between rainfall and DMI  
123 with malaria along the altitudinal gradient of our study locations using cross correlation  
124 functions [15]. Further details about the data and methods are presented in the Supplementary  
125 Data.

## 126 **Results**

127 Estimates for malaria regional synchrony (Table 1) were similar using SSA, Loess (Fig. 4A) and  
128 EMD (Fig. 4B) detrended time series. Malaria time series synchronicity was observed across the  
129 2-dimensional distance, and altitude, gradients, with all series in phase and with their maximum  
130 correlation observed at lag 0 (Fig. 4C), with minimum correlations well above 0.3 at lag 0 in the  
131 EMD detrended malaria data (Fig 4B, 4C, Table 1). For rainfall, synchrony estimates from the  
132 raw time series (Fig. 4D) and EMD (Fig. 4E) were very similar across the range of distances and  
133 altitudes studied (Fig. 4F). To estimate the smoothed correlogram of malaria (Fig. 4B) and  
134 rainfall (Fig. 4E) we employed only the EMD detrended time series since this procedure also  
135 allowed to filter out high frequency components in the time series, which can artificially increase  
136 time series synchrony by the emerging correlation expected from high frequency band

137 constraints. The smoothed correlograms for both malaria (Fig. 4B) and rainfall (Fig. 4E) were  
138 similar to the regional synchrony, as the 95% confidence envelope contained the smoothed  
139 correlogram along the range of studied distances in each case (Fig. 4B, 4E). Similarly, as  
140 expected under a Moran effect, the regional malaria and rainfall synchrony patterns were not  
141 statistically different (Table 1). Two-month lagged rainfall had the highest positive correlation  
142 with malaria, with a decreasing association as function of increasing elevation (Fig. 5A), a  
143 pattern also observed for an analysis based only on the EMD extracted seasonal malaria IMFs  
144 (Fig. 5B). The consideration of EMD extracted interannual malaria IMFs (Fig. 5C) showed the  
145 association between interannual rainfall and interannual malaria to have a maximum positive  
146 correlation when rainfall is 1 month lagged in relation with malaria, and a maximum negative  
147 correlation when rainfall is 4 month lagged in relation with malaria, suggesting a role for rainfall  
148 temporal variability in the synchronous malaria dynamics. The SSA detrended Malaria-DMI  
149 Cross Correlation Function (Fig. 5D) showed the positive association between these time series  
150 was maximum for up to 4 months of lagged DMI at altitudes over 1600 m. When the seasonal  
151 (Fig. 5E) and interannual (Fig. 5F) malaria IMF were correlated with DMI, the association up to  
152 4 months of lagged DMI showed to be robust at interannual scales and altitudes over 1600 m. In  
153 addition, the analysis with the IMFs also showed that DMI and seasonal components of malaria  
154 are associated at seasonal scales for 3 and 4 months of lagged DMI (Fig. 5E) and the association  
155 between DMI and malaria can be continuous along the altitudinal gradient given the emergence  
156 of significant patterns of association at altitudes below and above 1600 m (Fig. 5F). Patterns of  
157 association between malaria and DMI could be mediated by the impact of DMI on rainfall.  
158 DMI and rainfall have a correlation that decreases with altitude, which is maximized between 2  
159 and 6 months (Fig. 6A), where DMI has nil impacts on the seasonal components of rainfall (Fig.  
160 6B), but is positively associated with the interannual components of rainfall (Fig. 6C).

161

## 162 **Discussion**

163 Moran effects have seldom been observed in population dynamics [2, 3]. This could reflect the  
164 dominance of endogenous feedbacks over exogenous forcing in population dynamics [19]. For  
165 example, in diseases, a decaying synchrony with distance, or travelling waves of transmission,

166 have been described for both vector-borne diseases [20] and directly transmitted diseases [21]. In  
167 contrast, we found that both seasonal and interannual cycles of malaria have a non-decaying  
168 synchrony, both in 2-d distance and along an altitudinal gradient, at distances far greater than  
169 mosquito vector dispersal, which on average barely exceeds 2 km [22] or children movement in  
170 the area [23]. Moreover, the degree of synchrony in malaria time series is slightly above, yet not  
171 statistically different, from rainfall synchrony, as expected under a Moran effect [3].

172 A Moran effect in malaria transmission at the LVB could be explained by the monotonic  
173 dependence of *Plasmodium* parasite transmission on *Anopheles* vector density in endemic areas  
174 [4]. Mosquito population regulation is sensitive to the availability and stability of larval habitats  
175 [5, 24]. In fact, *Anopheles* vector density tracks rainfall variability in LVB in a regular fashion  
176 [12]. It takes about two months for malaria transmission to reach its peak following large rainfall  
177 events, roughly the total time of a few mosquito generations [25] including the parasite  
178 incubation period [26]. This probably implies a reactive response by mosquitoes to the transient  
179 creation of habitats by rainfall, assuming a density-dependent regulation [14], a pattern described  
180 in other species of mosquitoes vector of pathogens. Since *Anopheles* mosquitoes are ubiquitous  
181 in LVB [5, 12, 24], a synchronized amplification of their populations and malaria transmission  
182 following rainfall could explain the patterns of synchrony we report here. If this is the case, then  
183 the IOD, which has the strongest impact on rainfall at high altitudes according to climatic  
184 circulation models [8], could drive the Moran effect in malaria transmission along LVB probably  
185 by homogenizing rainfall synchrony across the altitudinal gradient, thus homogenizing weather  
186 conditions that increase mosquito productivity [24]. The existence of Moran effects in malaria  
187 transmission is a pattern that shows the non-trivial impacts of climatic variability on malaria  
188 epidemics. For example, the spatial extent of synchronous patterns in malaria transmission, i.e.,  
189 the maximum distance over which malaria synchrony is constant, could be used as indicator of  
190 the minimum spatial scale for interventions aimed at eliminating malaria from a given landscape.  
191 Thus, consideration of impacts by environmental variability on malaria transmission biology is  
192 required to increase robustness in the development and implementation of malaria control and  
193 elimination programs, to at least be prepared against surprises that can arise from climatic  
194 variability, one of the many aspects shaping the complexity of malaria transmission.

195

196 **References**

- 197 1. Liebhold A, Koenig WD, Bjørnstad ON. Spatial synchrony in population dynamics. Annual Review of  
198 Ecology Evolution and Systematics **2004**; 35:467-490.
- 199 2. Ranta E, Lundberg P, Kaitala V. Ecology of Populations. Cambridge: Cambridge University Press, **2006**.
- 200 3. Blasius B, Stone L. Ecology: Nonlinearity and the Moran effect. Nature **2000**; 406:846-847.
- 201 4. Smith DL, Drakeley CJ, Chiyaka C, Hay SI. A quantitative analysis of transmission efficiency versus  
202 intensity for malaria. Nat Commun **2010**; 1:108.
- 203 5. Fillinger U, Sonye G, Killeen GF, Knols BGJ, Becker N. The practical importance of permanent and  
204 semipermanent habitats for controlling aquatic stages of *Anopheles gambiae sensu lato* mosquitoes:  
205 operational observations from a rural town in western Kenya. Tropical Medicine & International Health  
206 **2004**; 9:1274-1289.
- 207 6. Drakeley CJ, Carneiro I, Reyburn H, et al. Altitude-Dependent and -Independent Variations in  
208 *Plasmodium falciparum* Prevalence in Northeastern Tanzania. Journal of Infectious Diseases **2005**;  
209 191:1589-1598.
- 210 7. Bødker R, Msangeni HA, Kisinza W, Lindsay SW. Relationship between the intensity of exposure to  
211 malaria parasites and infection in the Usambara Mountains, Tanzania. American Journal of Tropical  
212 Medicine and Hygiene **2006**; 74:716-723.
- 213 8. Anyah R, Semazzi F, Xie L. Simulated physical mechanisms associated with multi-scale climate  
214 variability over Lake Victoria Basin in East Africa. Monthly Weather Review **2006**; 134:3588-3609.
- 215 9. Hashizume M, Terao T, Minakawa N. The Indian Ocean Dipole and malaria risk in the highlands of  
216 western Kenya. Proceedings of the National Academy of Sciences of the United States of America **2009**;  
217 106:1857-1862.
- 218 10. Behera SK, Luo J-J, Masson S, et al. Paramount impact of the Indian Ocean Dipole on the East African  
219 short rains: A CGCM Study. J Climate **2005**; 18:4514-4530.
- 220 11. Saji NH, Goswami BN, Vinayachandran PN, Yamagata T. A dipole mode in the tropical Indian Ocean.  
221 Nature **1999**; 401:360-3.
- 222 12. Minakawa N, Sonye G, Mogi M, Githeko A, Yan GY. The effects of climatic factors on the distribution  
223 and abundance of malaria vectors in Kenya. J Med Entomol **2002**; 39:833-841.
- 224 13. Shanks G, Biomndo K, Hay S, Snow R. Changing patterns of clinical malaria since 1965 among a tea  
225 estate population located in the Kenyan highlands. Transactions of the Royal Society of Tropical  
226 Medicine and Hygiene **2000**; 94:253 - 255.
- 227 14. Chaves LF, Koenraadt CJM. Climate Change and Highland Malaria: Fresh Air for a Hot Debate. The  
228 Quarterly Review of Biology **2010**; 85:27-55.
- 229 15. Shumway RH, Stoffer DS. Time series analysis and its applications. New York: Springer, **2000**.
- 230 16. Ghil M, Allen MR, Dettinger MD, et al. Advanced spectral methods for climatic time series. Reviews  
231 of Geophysics **2002**; 40.
- 232 17. Huang NE, Shen Z, Long SR, et al. The empirical mode decomposition and the Hilbert spectrum for  
233 nonlinear and non-stationary time series analysis. Proceedings of the Royal Society of London Series a-  
234 Mathematical Physical and Engineering Sciences **1998**; 454:903-995.
- 235 18. Bjørnstad ON, Falck W. Nonparametric spatial covariance functions: Estimation and testing.  
236 Environmental and Ecological Statistics **2001**; 8:53-70.
- 237 19. Turchin P. Complex population dynamics. Princeton: Princeton University Press, **2003**.
- 238 20. Cummings DAT, Irizarry RA, Huang NE, et al. Travelling waves in the occurrence of dengue  
239 haemorrhagic fever in Thailand. Nature **2004**; 427:344-347.

- 240 21. Viboud C, Bjørnstad ON, Smith DL, Simonsen L, Miller MA, Grenfell BT. Synchrony, waves, and spatial  
241 hierarchies in the spread of influenza. *Science* **2006**; 312:447-451.
- 242 22. Silver JB. *Mosquito ecology: field sampling methods*. 3rd ed. New York: Springer, **2008**.
- 243 23. Prothero RM. *Migrants and Malaria*. London (UK): Longmans, **1965**.
- 244 24. Minakawa N, Omukunda E, Zhou G, Githeko A, Yan G. Malaria vector productivity in relation to the  
245 highland environment in Kenya. *American Journal of Tropical Medicine and Hygiene* **2006**; 75:448-53.
- 246 25. Bayoh MN, Lindsay SW. Effect of temperature on the development of the aquatic stages of  
247 *Anopheles gambiae sensu stricto* (Diptera : Culicidae). *Bulletin of Entomological Research* **2003**; 93:375-  
248 381.
- 249 26. Lindsay SW, Birley MH. Climate change and malaria transmission. *Annals of Tropical Medicine and*  
250 *Parasitology* **1996**; 90:573-588.

251

## 252 **Acknowledgements**

253 We thank R. Snow for providing hospital and meteorological data for Kericho. We also thank the  
254 staff at the Kendu Bay, Maseno, Kisii and Kapsabet hospitals for their help with data  
255 compilation. LFC, MH and NM had grant support to study synchrony patterns on malaria  
256 transmission at Lake Victoria Basin. LFC is a Gaikokuujin Fellow of Japan Society for the  
257 Promotion of Science.

258

259 **Figure Legends**

260 **Fig. 1 Data** (A) Malaria Time Series. (B) Rainfall. (C) Dipole Mode Index. (D) Trends (solid  
 261 lines for Loess, dashed lines for Singular Spectrum Analysis [SSA] and dotted lines for  
 262 Empirical Mode Decomposition[EMD]). There is no dashed line for Kisii and Kapsabet because  
 263 the SSA was unable to detect any trends. (E) Loess detrended Malaria time series. (F) SSA  
 264 detrended Malaria Time Series. (G) Malaria intrinsic mode functions, IMFs, with interannual  
 265 cycles. (H) Malaria IMFs with seasonal cycles. (I) Malaria IMFs with high frequency cycles.  
 266 Inset legends identify time series with colors. Color codes are shared by panels A, D, E, F, G, H,  
 267 I. IMFs were derived via an EMD for each time series.

268 **Fig. 2 Study Sites in Lake Victoria Basin, Western Kenya.** Kisumu ( $0^{\circ}6'S$   $34^{\circ}45'E$  Altitude =  
 269 1131 m); Kendu Bay ( $0^{\circ}24'05''S$ ,  $34^{\circ}39'56''E$ , Altitude = 1240 m); Maseno ( $0^{\circ}00'15''S$ ,  
 270  $34^{\circ}36'16''E$ , Altitude = 1500 m); Kisii ( $0^{\circ}40'S$ ,  $34^{\circ}46'E$ , Altitude = 1670 m); Kapsabet ( $0^{\circ}12'N$ ,  
 271  $35^{\circ}06'E$ , Altitude = 2000 m); Kericho ( $0^{\circ}23'55''N$ ,  $35^{\circ}15'30''E$ , Altitude = 2000 m). In the map  
 272 elevation is measured in meters, m, and indicated by gray. Location color indicates the data  
 273 available at each site ; blue (rainfall); green (disease) and red (disease and rainfall).

274 **Fig. 3 Rainfall Time Series Empirical Mode Decomposition** (A) Intrinsic mode functions,  
 275 IMFs, with interannual cycles; (B) IMFs with seasonal cycles; (C) IMFs with high frequency  
 276 cycles. Inset legends identify time series with colors.

277 **Fig. 4 Synchrony Analysis** (A) Malaria time series correlation at lag 0,  $r_0$ , as function of latitude  
 278 (Lat), longitude (Long) and two-dimensional distance [2D] between the studied localities. Colors  
 279 indicate the method employed to detrend the malaria time series employed to estimate  $r_0$ . (B) 2D  
 280 distance spline correlogram (3 edf) for the signal obtained by adding the seasonal and interannual  
 281 intrinsic mode functions from the empirical mode decomposition applied to the malaria time

282 series (C) Contour maps for temporal cross-correlations between the Empirical Mode  
283 Decomposition [EMD] detrended malaria time series (D) Rainfall time series correlation at lag 0,  
284  $r_0$ , as function of latitude (Lat), longitude (Long) and 2D distance between the studied localities.  
285 (E) 2D distance spline correlogram (2 edf) for the signal obtained by adding the seasonal and  
286 interannual intrinsic mode functions from the empirical mode decomposition applied to the  
287 rainfall time series. (F) Contour maps for temporal cross-correlations among the Rainfall time  
288 series. In A, B, D, and E Synch is the estimated regional synchrony obtained with each method.  
289 In B and E dotted lines indicate the 95% confidence envelope for the smoothed correlation  
290 function, solid line, obtained with 1000 data permutations. In C and F, the y axis represents the  
291 lag for the cross correlation and the x axis represents the 2D distance. Values in the contour lines  
292 are correlations, which are significantly different from 0 when their absolute value is above  
293 0.075 ( $P < 0.05$ ).

294 **Fig. 5 Time scale impacts of Rainfall and Indian Ocean Dipole on malaria synchrony across**  
295 **an altitude gradient** (A) Singular Spectrum analysis detrended malaria time series (SSA  
296 Malaria) correlation with Rainfall (B) Seasonal malaria Intrinsic Mode Function, IMF,  
297 correlation with Seasonal Rainfall IMF (C) Interannual malaria IMF correlation with Interannual  
298 Rainfall IMF (D) SSA detrended malaria correlation with Dipole mode index (DMI) (E)  
299 Seasonal malaria IMF, correlation with DMI (F) Interannual malaria IMF correlation with DMI.  
300 IMFs for each malaria time series were obtained by empirical mode decompositions. In all  
301 panels the x axis represents the lag for the cross correlation and the y axis represents the site  
302 altitude. Values in the contour lines are correlations, which are significantly different from 0  
303 when their absolute value is above 0.075 ( $P < 0.05$ ).

304 **Fig. 6 Time Scale association between Rainfall and Dipole mode Index (DMI).** (A) Rainfall  
305 correlation with DMI (B) Seasonal rainfall Intrinsic Mode Function, IMF, correlation with DMI  
306 (C) Interannual rainfall IMF, correlation with DMI. IMFs for each malaria time series were  
307 obtained by empirical mode decompositions. The x axis represents the lag for the cross  
308 correlation and the y axis represents the site altitude. Values in the contour lines are correlations,  
309 which are significantly different from 0 when their absolute value is above 0.075 ( $P < 0.05$ ).

Figure 1  
[Click here to download high resolution image](#)

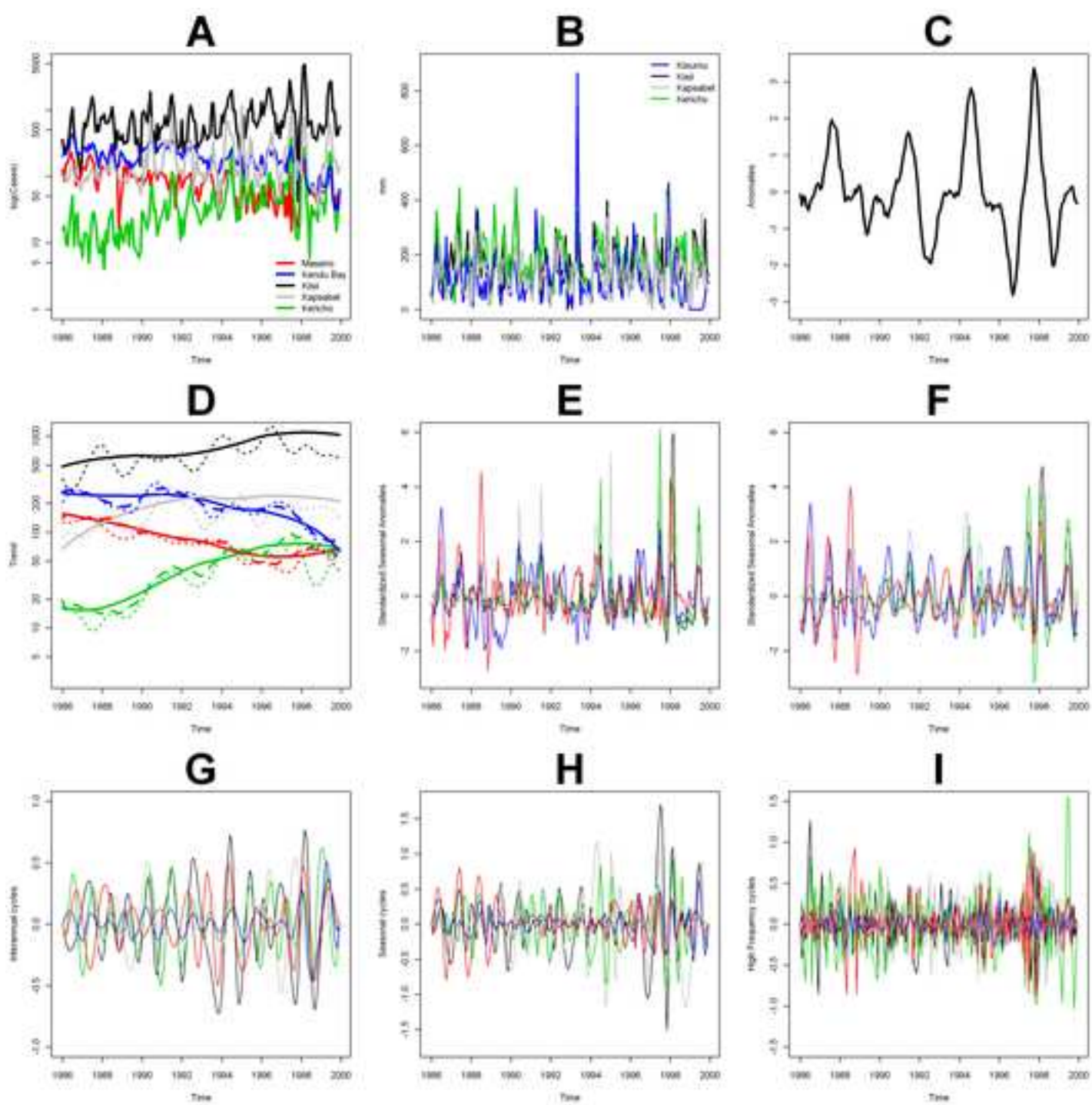


Figure 2  
[Click here to download high resolution image](#)

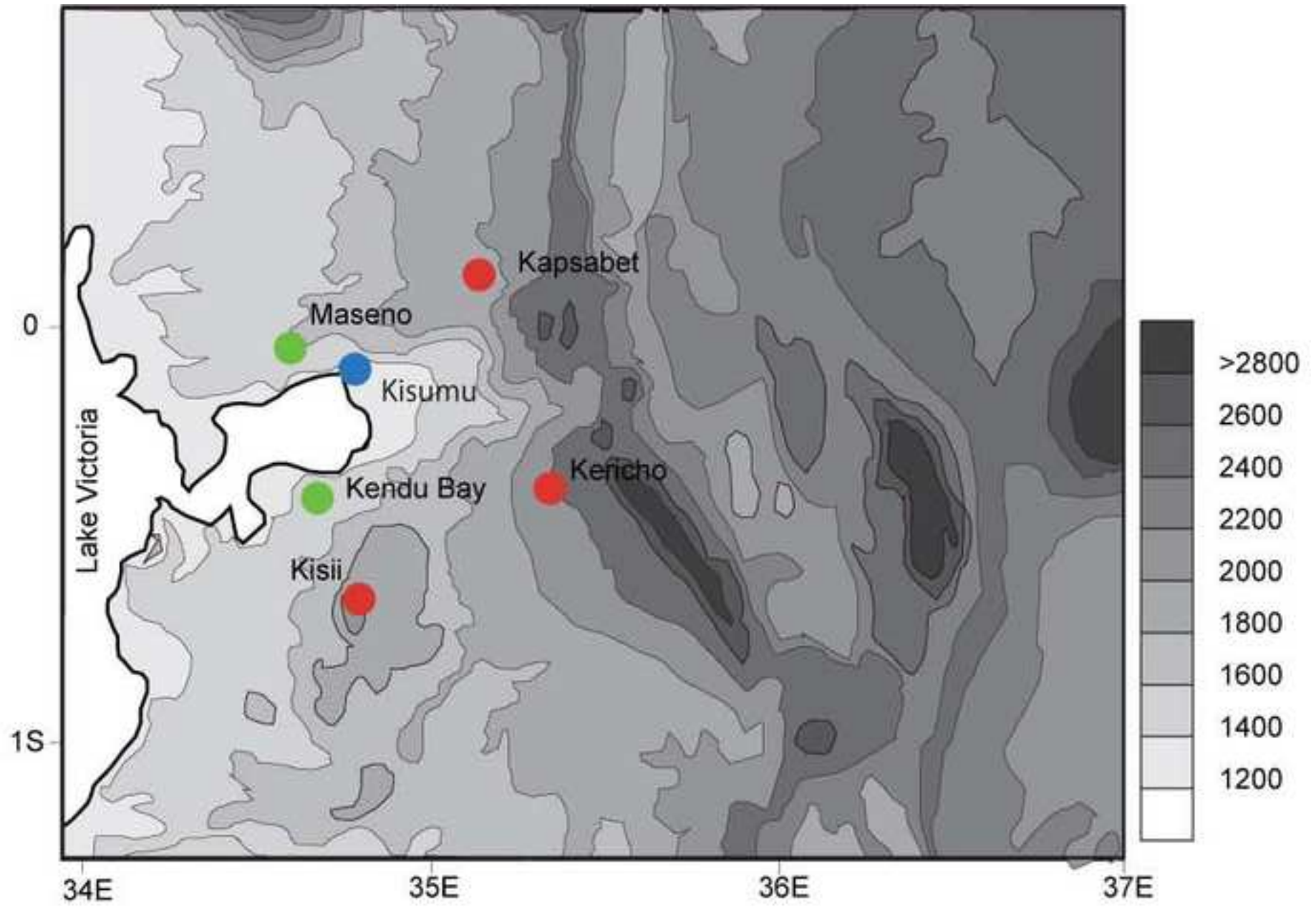


Figure 3  
[Click here to download high resolution image](#)

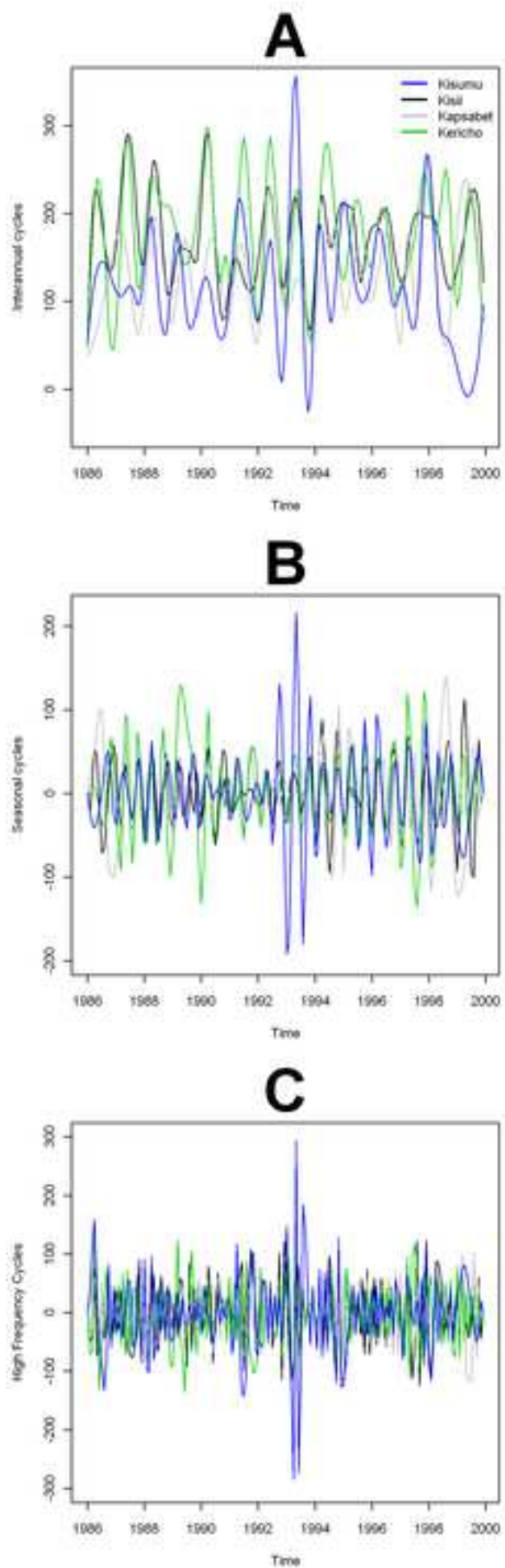


Figure 4  
[Click here to download high resolution image](#)

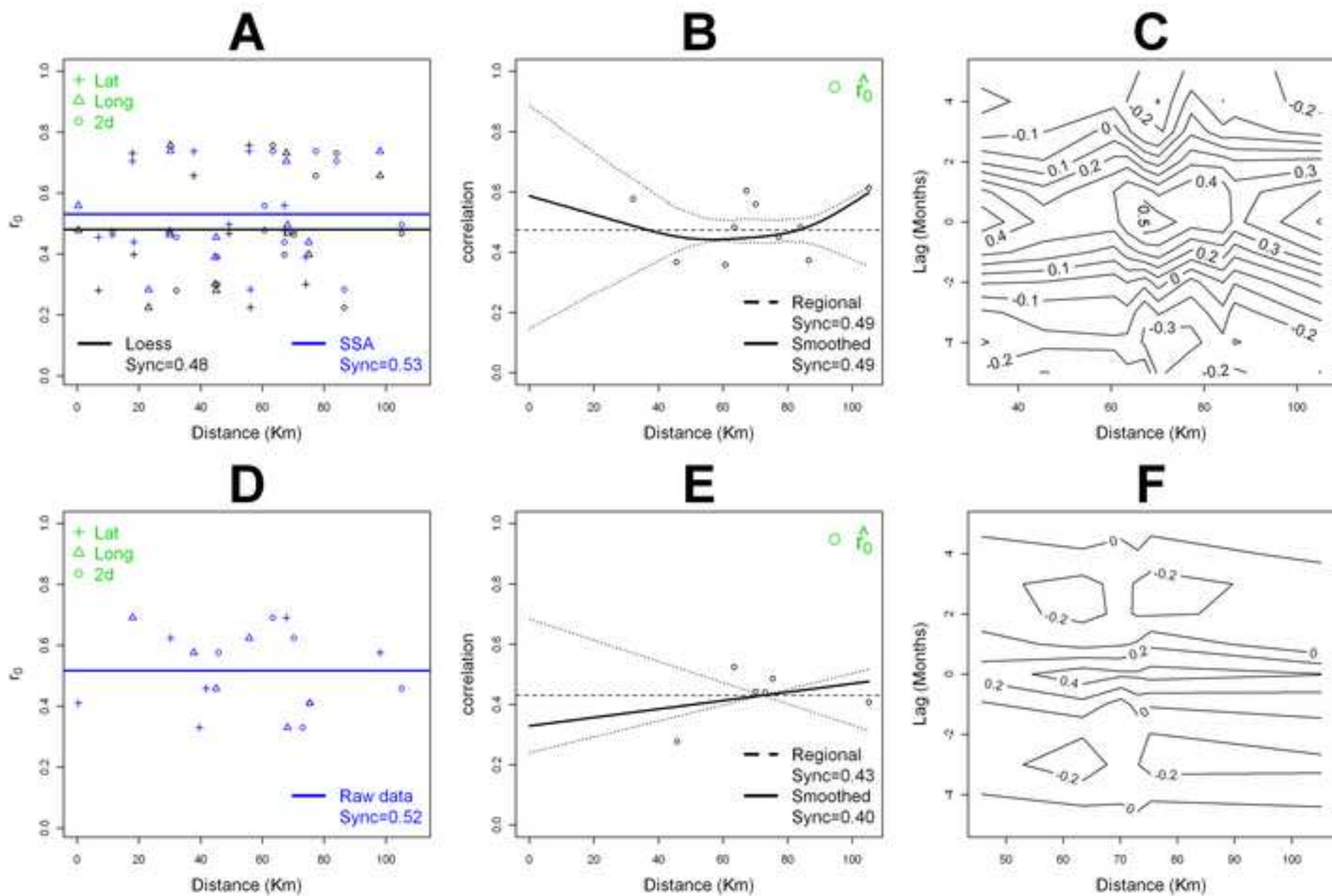
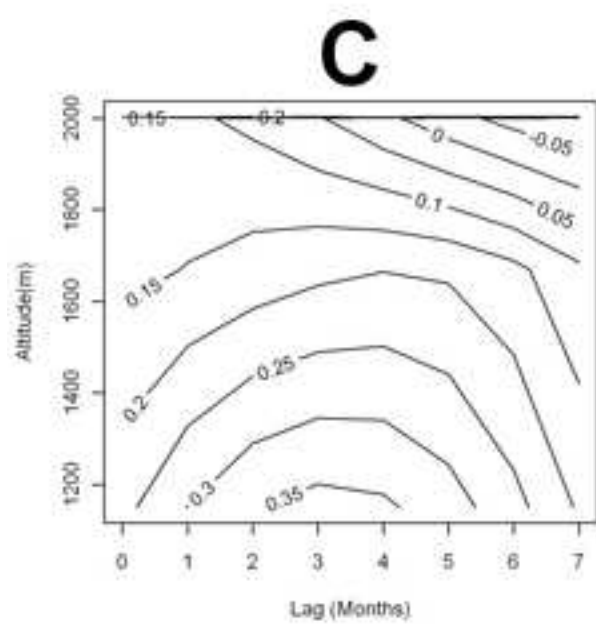
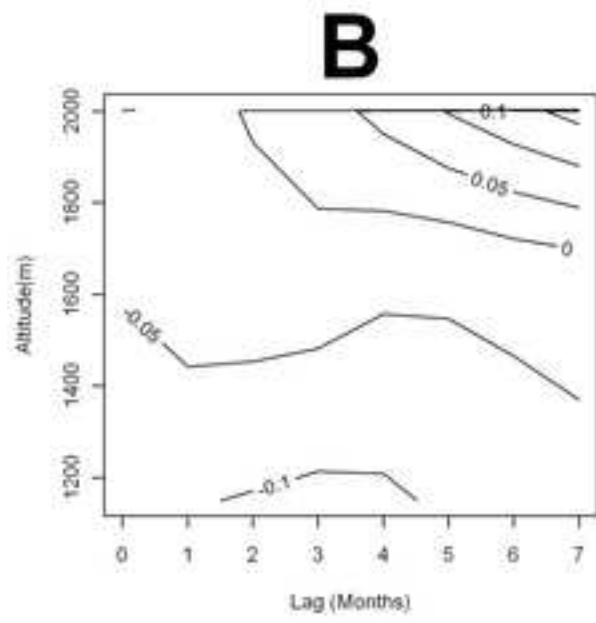
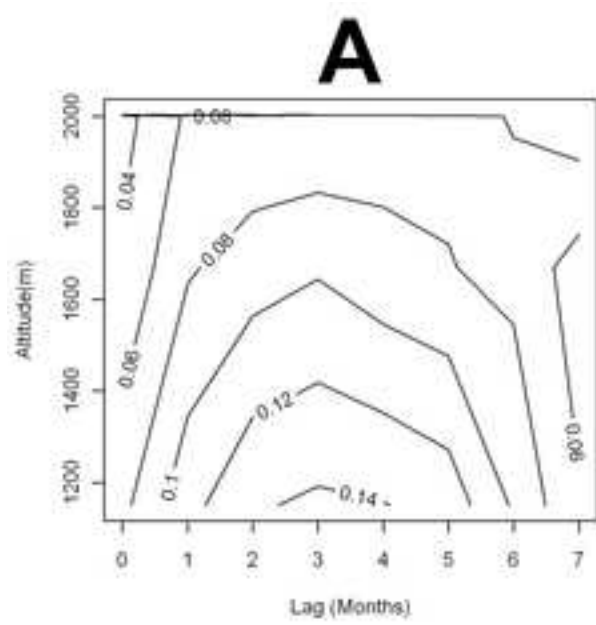




Figure 6  
[Click here to download high resolution image](#)



**Table 1.** Confidence limits for the regional synchrony estimates. 95% confidence limits were estimated from the standard error of maximum likelihood estimates for the regional synchrony.

<b>Time Series</b>	<b>Mean <math>\pm</math> S.E.</b>	<b>95% Confidence limits</b>
Malaria-LOESS	$0.48 \pm 0.06$	0.34 - 0.61
Malaria-SSA	$0.53 \pm 0.05$	0.42 - 0.64
Malaria-EMD	$0.49 \pm 0.03$	0.42 - 0.56
Rainfall-Raw Data	$0.52 \pm 0.06$	0.37- 0.66
Rainfall-EMD	$0.43 \pm 0.03$	0.34 - 0.51

## **Supplementary data**

### **Detailed Methods**

#### **Software**

All statistical analyses were performed using the statistical software R[1].

#### **Time series detrending methods**

##### *Loess*

This is a well established procedure to remove non-linear trends from time series data [2]. A non-parametric trend is fitted to the time series using local polynomials regression fits, Loess, which is then subtracted from the original series [3]. For the synchrony analysis, such residuals are then standardized to be normal and with a variance of one [2].

##### *Singular spectrum analysis (SSA)*

This non-parametric technique separates trends and oscillatory components from noise in a time series [4]. The method consists in the computation of the eigenvalues and eigenvectors from a covariance matrix [**M**] whose element  $m_{ij}$  is the covariance between lags  $i$  and  $j$ . The projection of the time series on the eigenvectors (the principal components of the matrix) reconstructs the pattern of variability associated with the selected eigenvalue, resulting in a de-noised time series [4]. The eigenvalues themselves indicate how much variance is accounted for by the different components [4].

##### *Empirical Mode Decomposition (EMD)*

This technique decomposes time series into trends and oscillatory components. Briefly, a time series goes through an iterative sifting process which decomposes the time series into a sum of intrinsic mode functions (IMF). The algorithm to extract IMFs is as follows: (i) Envelopes are built by joining through a cubic spline all the maxima (upper envelope) and minima (lower envelope); (ii) the mean of the two envelopes is subtracted from the time series; and (iii) the

process is repeated until an IMF is obtained. IMFs should satisfy the assumption of a narrow band (which is fulfilled when the number of zero crossings and extrema are either equal or differ by one) and the mean of its upper and lower envelopes, equals zero (which renders impossible unwanted fluctuations expected by asymmetric waveforms). The process of extracting IMFs can be repeated on the residuals from each IMF extraction until all cyclic components are extracted and the final residuals represent a trend for the data. Further details and a mathematically rigorous explanation are presented by Huang et al [5]. Regarding our data, we extracted three IMFs and the trend (Fig. 1D) from the malaria time series, each IMF corresponding to interannual cycles (Fig. 1G), seasonal cycles (Fig. 1H) and high frequency cycles (Fig. 1I). For the rainfall time series we only extracted two IMFs, because the extraction of a third IMF did not lead to the separation of trends, and the trends lacked any noticeable non-cyclical pattern (Fig. 3A). Like the malaria time series, the rainfall time series also had seasonal (Fig. 3B) and high frequency components (Fig. 3C). For the EMD malaria data were log-transformed, in order to minimize signal interference.

### **Spline Correlogram**

We employed spline correlograms to study rainfall and malaria synchrony. This technique can be used to study the spatio-temporal autocorrelation among populations. Basically, smoothing splines are used to generate a functional correlogram, i.e., an assumption free and smooth function depicting spatial autocorrelation, among several time series, which depends on distance. Given the low number of time series, (5 for malaria and 4 for rainfall, numbers rendering impossible a bootstrap), we generated a null distribution from the estimator by computing spline correlograms from random time series. The random time series were constructed by sampling without replacement the detrended, and also high frequency filtered, time series, i.e., we analyzed time series without trends to ensure a stationary mean and, series without high frequency components to avoid the spurious correlations that can be expected when these components are considered. This procedure was repeated 1000 times to extract the 2.5% and 97.5 % quantiles of the null distribution, which correspond to the 95% confidence envelope of the spline correlogram [6]. For the smoothing of the 5 malaria time series we employed 3 degrees of freedom (edf), and to make a reliable comparison we used 2 edf given that we only had 4 rainfall time series.

## Cross Correlation Function

Cross correlation function, CCF, is formally defined as the ratio between the cross-covariance function of two time series divided by the square root of the product of each series variance, and represents the association between time series as function of time [2].

### References

1. R DCT. R: A language and environment for statistical computing  
Vienna, Austria: R Foundation for Statistical Computing, **2011**.
2. Shumway RH, Stoffer DS. Time series analysis and its applications. New York: Springer, **2000**.
3. Ranta E, Lundberg P, Kaitala V. Ecology of Populations. Cambridge: Cambridge University Press, **2006**.
4. Ghil M, Allen MR, Dettinger MD, et al. Advanced spectral methods for climatic time series. *Reviews of Geophysics* **2002**; 40.
5. Huang NE, Shen Z, Long SR, et al. The empirical mode decomposition and the Hilbert spectrum for nonlinear and non-stationary time series analysis. *Proceedings of the Royal Society of London Series a-Mathematical Physical and Engineering Sciences* **1998**; 454:903-995.
6. Bjørnstad ON, Falck W. Nonparametric spatial covariance functions: Estimation and testing. *Environmental and Ecological Statistics* **2001**; 8:53-70.